How Strong ENSO Events Affect Tropical Storm Activity over the Western North Pacific*

BIN WANG

Department of Meteorology, and International Pacific Research Center, University of Hawaii at Manoa, Honolulu, Hawaii

JOHNNY C. L. CHAN

Department of Physics and Materials Science, City University of Hong Kong, Hong Kong, China

(Manuscript received 7 March 2001, in final form 5 December 2001)

ABSTRACT

An analysis of 35-yr (1965–99) data reveals vital impacts of *strong* (but not moderate) El Niño and La Niña events on tropical storm (TS) activity over the western North Pacific (WNP). Although the total number of TSs formed in the entire WNP does not vary significantly from year to year, during El Niño summer and fall, the frequency of TS formation increases remarkably in the southeast quadrant (0°–17°N, 140°E–180°) and decreases in the northwest quadrant (17°–30°N, 120°–140°E). The July–September *mean location* of TS formation is 6° latitude lower, while that in October–December is 18° longitude eastward in the strong warm versus strong cold years. After the El Niño (La Niña), the early season (January–July) TS formation in the entire WNP is suppressed (enhanced). In strong warm (cold) years, the mean TS *life span* is about 7 (4) days, and the mean number of days of TS *occurrence* is 159 (84) days. During the fall of strong warm years, the number of TSs, which recurve northward across 35°N, is 2.5 times more than during strong cold years. This implies that El Niño substantially enhances poleward transport of heat–moisture and impacts high latitudes through changing TS formation and tracks.

The enhanced TS formation in the SE quadrant is attributed to the increase of the low-level shear vorticity generated by El Niño–induced equatorial westerlies, while the suppressed TS generation over the NW quadrant is ascribed to upper-level convergence induced by the deepening of the east Asian trough and strengthening of the WNP subtropical high, both resulting from El Niño forcing. The WNP TS activities in July–December are noticeably predictable using preceding winter–spring Niño-3.4 SST anomalies, while the TS formation in March–July is exceedingly predictable using preceding October–December Niño-3.4 SST anomalies. The physical basis for the former is the phase lock of ENSO evolution to the annual cycle, while for the latter it is the persistence of Philippine Sea wind anomalies that are excited by ENSO forcing but maintained by local atmosphere–ocean interaction.

1. Introduction

Since the mid-1980s, the interannual variations of tropical cyclone (TC) activity over different ocean basins have received increasing attention (see the review in Landsea 2000). Among these, most studies focus on the effect of the El Niño–Southern Oscillation (ENSO). A rich background of literature can be found in the past 20 years on the ENSO influence on tropical cyclone formation over the western North Pacific (WNP), a vast region spanning from 120°E to the date line and from the equator to 30°N. Although there is a general consensus that El Niño affects the location of the tropical storm (TS) formation in the WNP, the results are described in a qualitative way and somewhat controversial due to the differences in analysis procedures, datasets, and definitions of El Niño events used by different authors. While Atkinson (1977), Chan (1985, 2000), Dong (1988), Wu and Lau (1992), and others have noticed that the TSs tend to form more eastward during the El Niño, they did not scrutinize seasonal differences. They reached a common conclusion that the number of TS formations over the WNP is less than normal during El Niño years. Lander (1993) challenged this conclusion and pointed out that, in spite of the eastward displacement of the genesis region of tropical cyclones during El Niño, the observed annual tropical cyclone totals in the WNP are virtually uncorrelated with ENSO indices. This latter result corroborates with Ramage and Hori

* School of Ocean and Earth Science and Technology Publication Number 5950 and International Pacific Research Center Publication Number 149.

Corresponding author address: Dr. Bin Wang, Department of Meteorology, University of Hawaii at Manoa, 2525 Correa Rd., Honolulu, HI 96825.
E-mail: bwang@soest.hawaii.edu

(1981) but contradicts with the prevailing notion in the forecast community that El Niño years are supposed to have fewer tropical cyclones in the WNP (e.g., Japanese Meteorological Agency 1991). This calls for a revisit of this issue using the longest possible available dataset. In addition, the issue is not whether El Niño has an impact on the TS formation location, but is how much is the El Niño's impact quantitatively.

The analysis performed by Kang et al. (1995) and Chen et al. (1998) added new findings. The EOF analysis of the genesis region performed by Kang et al. (1995) shows a large-scale picture of the shift of the genesis locations within the WNP domain. Chen et al. (1998) noticed the difference in total tropical cyclone activity between June–August (JJA) (mainly northward shift of the TS formation during El Niño) and September–November (SON, hereafter all ranges of months will follow this abbreviation style) (eastward shift). Their conclusion was based on a shorter dataset (16 yr) and using a moderate Niño-3 SST anomaly (0.5°C) as a criterion for stratifying warm/cold events without considering the differences between the strong and weak ENSO events. In addition, they used specific features in the anomalous 850-hPa geopotential height field as complementary criteria to define warm and cold years. Such a procedure would blend the effects of the local circulation and ENSO.

In the previous studies, attention was primarily paid to the TC generation or TS formation, except for that by Chan (1994) who identifies the regions of large variability in TC tracks and attempted to forecast the TC movement over these regions by using observed wind anomaly patterns in the previous seasons. To date, changes in the TS tracks, TS life spans, and the frequency of TS occurrence between the El Niño and La Niña years have not been documented. In this study, we aim at a methodical exploration of all these aspects of the variability of TC activity and at quantification of the location and frequency of TS formation (or tropical cyclone intensification).

A number of mechanisms have been proposed to explain how ENSO impacts TS formation over the WNP, including those through changing 1) the vertical shear (Gray 1984), 2) the WNP SST (Li 1988), 3) the Walker circulation, and 4) the WNP monsoon trough. Chan (1985) suggested that during El Niño years, an anomalous Walker circulation is set up with rising motion in the central part of the equatorial Pacific and sinking motion in the western part that tends to suppress convection, and hence, tropical cyclone activity over the WNP. In explaining the Geophysical Fluid Dynamics Laboratory (GFDL) model results, Wu and Lau (1992) considered that the sinking motion over the Indonesian Archipelago weakens the WNP monsoon trough and associated westerlies, which is accompanied by decreasing TS activity over the WNP. Lander (1994) and Chen et al. (1998) attributed the eastward shift of the genesis area to an eastward extension of the monsoon trough axis in the WNP.

The notion concerning El Niño's impacts via a shift in the Walker circulation is more relevant to explain the late season (OND) eastward displacement of the TS formation region, because in the late season TSs tend to form close to the equator and so are the ENSO-induced low-level circulation anomalies. Since the TS–ENSO relationship varies with season, the mechanisms operating during the peak season (JAS) and early season (AMJ) of the El Niño (La Niña) years could be different from that found in the late season. Further explanation of ENSO effects on WNP TS activity should particularly focus on how ENSO affects 1) the peak season and 2) the early season TS activity. No explanation has been attempted to the above questions except Chen et al. (1998) who pointed out a close link between the interannual variation of TC genesis frequencies and a summer teleconnection wave train in the WNP. They argued that the interannual variation of the TC generation over the WNP is caused by the tropical Pacific SST anomalies through the formation of this anomalous wave train.

Various statistical schemes and predictors have been proposed to forecast the WNP TS formation (e.g., Chan et al. 1998). Yet, the physical basis for such a practice has rarely been discussed. In the present paper, we explore what aspects of TS activity are more predictable than others in terms of the relationships with the Pacific SST anomalies, and what are the physical bases for such predictabilities.

This paper is arranged into six sections. Section 2 describes the data and analysis strategy. Section 3 discusses to what extent and what properties of TS activity relate to SST anomalies over the equatorial Pacific. Section 4 elucidates how equatorial Pacific SST anomalies affect WNP TS activity. Section 5 discusses the physical basis for predicting TS activity using precursors in the anomalous SST field. The last section presents a summary.

2. Data and analysis procedure

a. Datasets

Best-track data of tropical cyclones (position and intensity) for the period 1965–99 are obtained online at the Joint Typhoon Warning Center Web site (www.npmoc.navy.mil/jtwc.html). The starting time is chosen to be 1965 when satellite monitoring of weather events first became routine so that no tropical cyclone would be missed. To minimize subjectivity in the identification of weak systems, only tropical cyclones that reached at least TS intensity (maximum sustained winds $\geq$17 m s^{-1}) are included in the data sample. Choice of TS intensity as a criterion for measuring TC intensification is quite arbitrary. Nevertheless, such a measure is believed to be representative of the TC intensification, meanwhile it may lessen the errors possibly arising from

1) the gradual increase in quality and coverage of satellite imagery, 2) the refinement of the satellite analysis technique (Dvorak 1975, 1984), and 3) the termination of the aircraft reconnaissance in 1987.

The SST anomalies in the different Niño regions are extracted online at the Climate Prediction Center Web site. Winds and vertical velocity fields used to understand the variability in TS activities are from the National Centers for Environmental Prediction–National Center for Atmospheric Research (NCEP–NCAR) reanalyses (www.cdc.noaa.gov/cdc/reanalysis) (Kalnay et al. 1996). Since the relationship between the TS activity and Pacific SST depends on the location of SST anomalies (SSTAs), we tested three major indices: the Niño-3 (5°S–5°N, 90°–150°W), Niño-3.4 (5°S–5°N, 120°–170°W), and Niño-4 (5°S–5°N, 150°W–160°E) SSTA. It is found that the Niño-3.4 SSTA is better correlated with the overall TS activity. This is because the occurrence of organized convection depends on the total SST and SST gradient rather than the SST anomaly itself (Graham and Barnet 1987; Wang and Li 1993). The central Pacific is a region where SST gradients are largest among the three Niño regions, and the background SST is also higher than that in the eastern Pacific. Thus, tropical convection is more sensitive to the SST variability in the Niño-3.4 than in the Niño-3 region. The Niño-3.4 SSTA is also better than the Niño-4 SSTA because in the Niño-4 region, SST variability and the background SST gradient are considerably weaker than those in the Niño-3.4 region. In this paper, we used Niño-3.4 SSTA to stratify El Niño (La Niña) strength.

b. Classification of warm (cold) seasons and El Niño (La Niña) years

Although tropical storms can occur throughout the year, the frequency in February is an absolute minimum and JFM is the least frequent TS season (Lander 1994). Based on the seasonal distribution of TS formation, we focus on three TS seasons: early season (AMJ), peak season (JAS), and late season (OND).

The sign and amplitude of equatorial Pacific SSTA during the same year varies with season. Figure 1 indicates that the early season SSTAs, in many years, differ considerably from the corresponding peak and late seasons. During El Niño developing years (e.g., 1965, 1968, 1972, 1976, 1982, 1986, and 1997), the early season SST is often near normal, whereas in the late season SST anomaly often reaches its peak. In the years after the mature phase of El Niño such as in 1970, 1983, 1992, 1995, and 1998, the SSTAs in the preseason are positive but turn to negative in the late season. Thus, it is not meaningful to classify preseason TS activity simply according to El Niño or La Niña years. Normally, the peak and late season SST anomalies have the same sign, but the amplitudes in the late season are considerably larger.

In view of the seasonal dependence, we stratify seasonal mean SSTA into five categories: strong warm (SSTA $>$ 1 std dev, or 1σ), moderate warm ($0.4\sigma <$ SSTA $\leq 1\sigma$), normal ($-0.4\sigma \leq$ SSTA $\leq 0.4\sigma$), moderate cold ($-1\sigma \leq$ SSTA $< -0.4\sigma$), and strong cold (SSTA $< -1\sigma$). In classification of El Niño or La Niña *years*, one may use the peak season SSTA because the stratification is the same if one uses the SSTA averaged for the entire TS season from April to December. The results of stratification are listed in Table 1.

Figure 2 displays the latitudinal and seasonal distribution of the frequency of TS formation for the five-category years. In the early season, tropical storms tend to form more frequently in the strong warm years in contrast to strong cold years. In the peak season, the latitude of formation during the strong warm years is considerably lower than that during the strong cold years. In the late season, no obvious difference in the formation latitude can be found, but the longitude of TS formation differs considerably as will be presented shortly. These results point to the necessity of performing analyses according to *TS seasons.* Also seen from Fig. 2 is that the frequencies of TS formation during the moderate warm and moderate cold years appear to resemble that of the normal years. This suggests that perhaps only when the Niño-3.4 SSTA has considerable amplitude ($\sim 1\sigma$) is the impact of SSTA on the latitude of TS formation evident. In the following analysis, composites will be primarily made for the strong warm and cold categories.

3. Contemporaneous relationship between TS activity and equatorial Pacific SSTAs

TS activity is measured by the following five parameters: 1) locations of TS formation (defined as the time when an intensifying tropical cyclone first reaches tropical storm intensity, i.e., maximum sustained winds ≥ 17 m s^{-1}), which measures the degree of TC intensification; 2) number of TS formations; 3) TS life span defined by the total length of time from the formation of TS to the moment when its intensity drops below TS intensity; 4) frequency of TS occurrence defined by the total number of days of TS occurrence; and 5) tracks of TSs.

a. Locations of TS formation

Figures 3–5 display positions of the TS formation for the strong warm and strong cold episodes during each TS seasons. A common feature to all three seasons is the prominent east–west shift between the warm and cold years, confirming previous findings (Chan 1985; Dong 1988; and many others). In the peak TS season, in addition to the zonal difference, a pronounced north–south difference is evident as noted by Chen et al. (1998). To test for statistical significance, we divide the tropical WNP (5°–30°N, 120°E–180°) into subregions according to seasons. For the early and peak seasons, 140°E serves as a boundary between the east and west

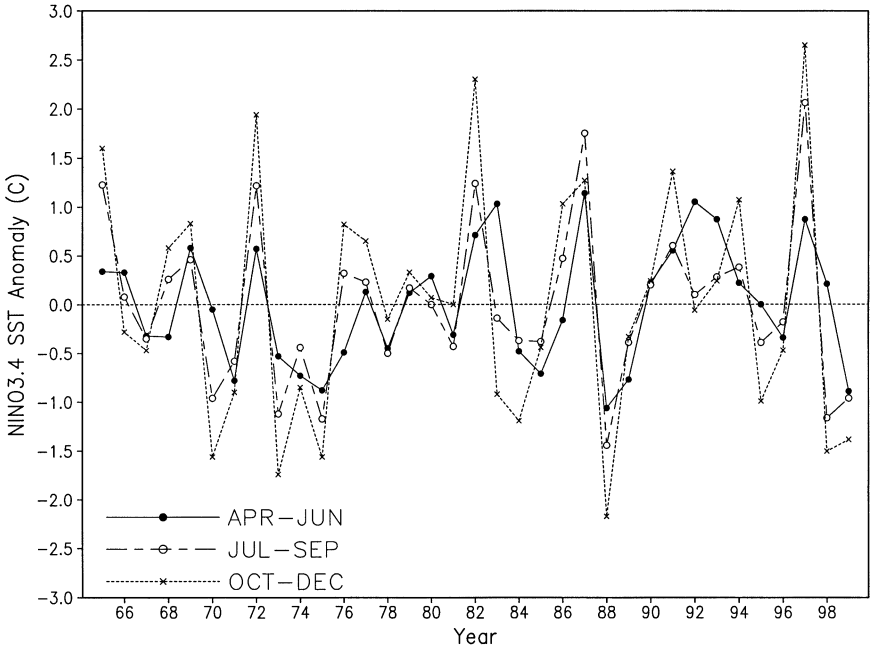

FIG. 1. Niño-3.4 SSTA time series averaged for the early (AMJ), peak (JAS), and late (OND) TS seasons.

(Figs. 3 and 4), while for the late season, 150°E is used as the border (Fig. 5). Such a division is in accord with the fact that the mean formation longitude in the late season is more eastward. Furthermore, for the peak season, 17°N is used to divide the WNP into northern and southern regions, resulting in four subregions (Fig. 4).

Table 2 shows contingency tables for observed numbers of TS formation. The chi-square test indicates the differences for the peak and late seasons are significant at the 1% level (the null hypothesis being no relationship between SSTA and TS formation numbers). During the peak season, the formation numbers show remarkable differences in the northwest (NW) and southeast (SE) quadrants of the WNP. In the SE quadrant (5°–17°N, 140°E–180°), the five warm years have 31 TS formations while the six cold years have only 2 (Fig. 4). In the NW quadrant (17°–30°N, 120°–140°E), the situation reverses with 28 TSs forming during the cold years while only 7 form during the warm years. In addition, about 75% of the TSs formed north of 17°N during the cold years, while 74% formed south of the 17°N during the warm years (Table 2b). In the late season, no TS formed east of 150°E in the cold years, whereas 60% formed in the same region during the warm years (Table 2c; Fig. 5). Over the South China Sea, the number of TS formations in the cold years (18) is 2.5 times that in the warm years (7).

To quantify the change in location, we examine mean locations of TS formation for each season (year), which are presented in Fig. 6. Statistical significances for each

TABLE 1. Stratification of five categories of seasons based on the std dev of the seasonal mean Niño-3.4 SSTAs.

	Preseason AMJ	Peak season JAS	Late season OND	Peak–late season Jul–Dec
Strong warm (>1 std dev)	1982, 1983, 1987, 1992, 1993, 1997	1965, 1972, 1982, 1987, 1997	1965, 1972, 1982, 1987, 1991, 1997	1965, 1972, 1982, 1987, 1997
Moderate warm (0.4 std dev, 1 std dev)	1965, 1966, 1969, 1972, 1980, 1991	1969, 1986, 1991, 1994	1968, 1969, 1976, 1977, 1986, 1994	1968, 1969, 1976, 1977, 1986, 1991, 1994
Normal (−0.4 std dev, 0.4 std dev)	1970, 1977, 1979, 1986, 1990, 1994, 1995, 1998	1966, 1968, 1976, 1977, 1979, 1980, 1983, 1990, 1992, 1993, 1996	1966, 1967, 1978, 1979, 1980, 1981, 1985, 1989, 1990, 1992, 1993, 1996	1966, 1978, 1979, 1980, 1981, 1989, 1990, 1992, 1993, 1996
Moderate cold (1 std dev, −0.4 std dev)	1967, 1968, 1973, 1976, 1978, 1981, 1984, 1996	1967, 1971, 1974, 1978, 1981, 1984, 1985, 1989, 1995	1971, 1974, 1983, 1984, 1995	1967, 1971, 1974, 1983, 1984, 1985, 1995
Strong cold (<−1 std dev)	1971, 1974, 1975, 1985, 1988, 1989, 1999	1970, 1973, 1975, 1988, 1998, 1999	1970, 1973, 1975, 1988, 1998, 1999	1970, 1973, 1975, 1988, 1998, 1999
Standard division	0.62	0.82	1.20	1.00

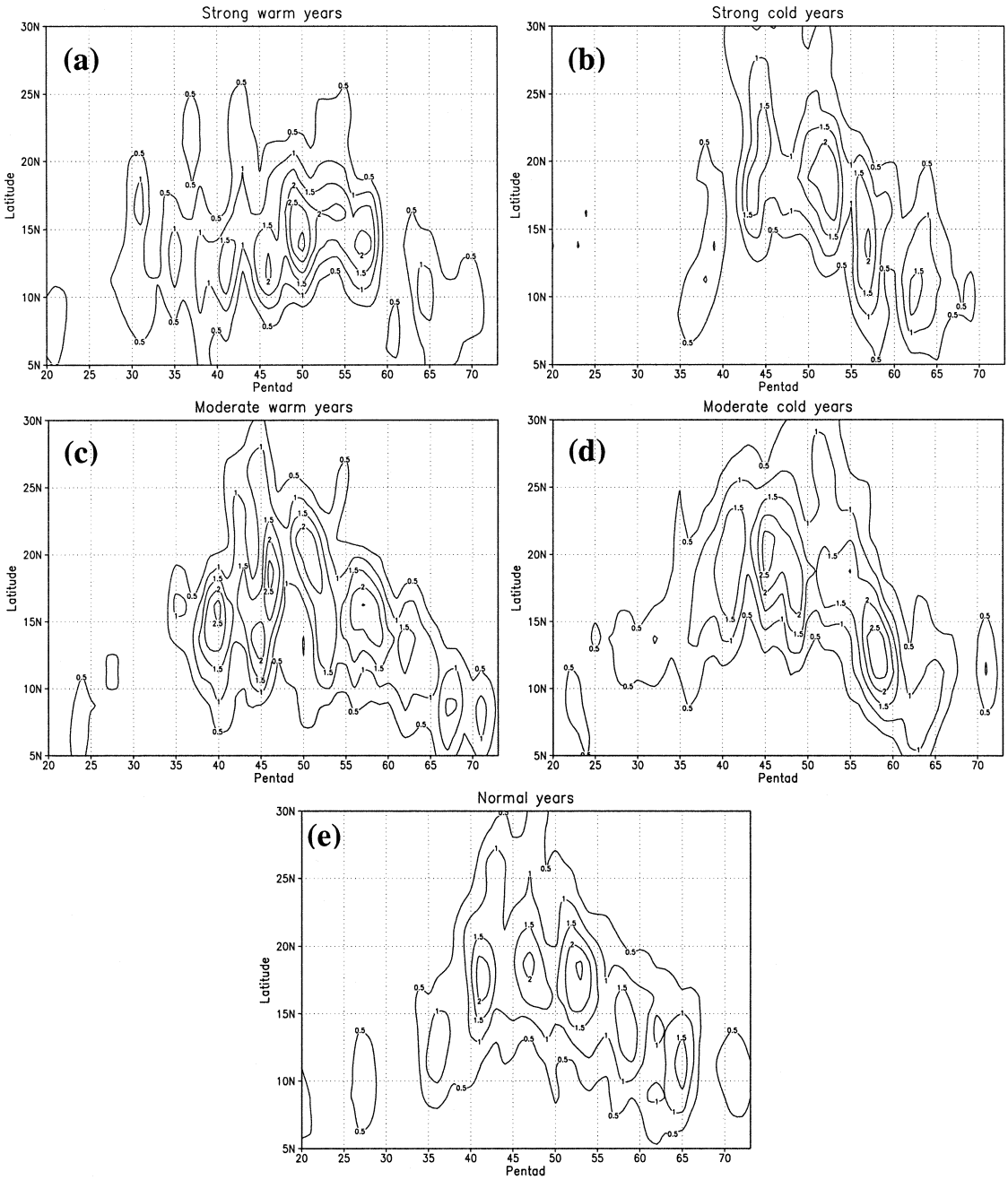

FIG. 2. Frequency of TS formation as a function of lat and time (pentad) for (a) strong warm, (b) strong cold, (c) moderate warm, (d) moderate cold, and (e) normal years. The definitions for five categories of SSTA are the same as that defined by JAS SSTA as shown in Table 1. The unit for contours is 0.1 per pentad.

category mean were tested by a two-sample *t* test (Wilks 1995). The null hypothesis is that the mean formation latitude (or longitude) averaged for each anomalous category is the same as that of the normal year category. The results (Table 3) show that for the peak and late season (July–December) the moderate warm or moderate cold years do not differ significantly from the normal years; only the strong warm and strong cold years differ significantly from those of the normal years. This conclusion is generally valid for the peak or late season alone.

During the peak season, the mean formation locations in the strong warm years are all south of 16°N, while those in the cold years are all north of 20°N (Fig. 6a). Their mean latitudes differ by 6°. During the late season, the locations of TS formation between the strong warm and cold years are well separated in the east–west direction by about 18° longitude (Fig. 6b). For the entire

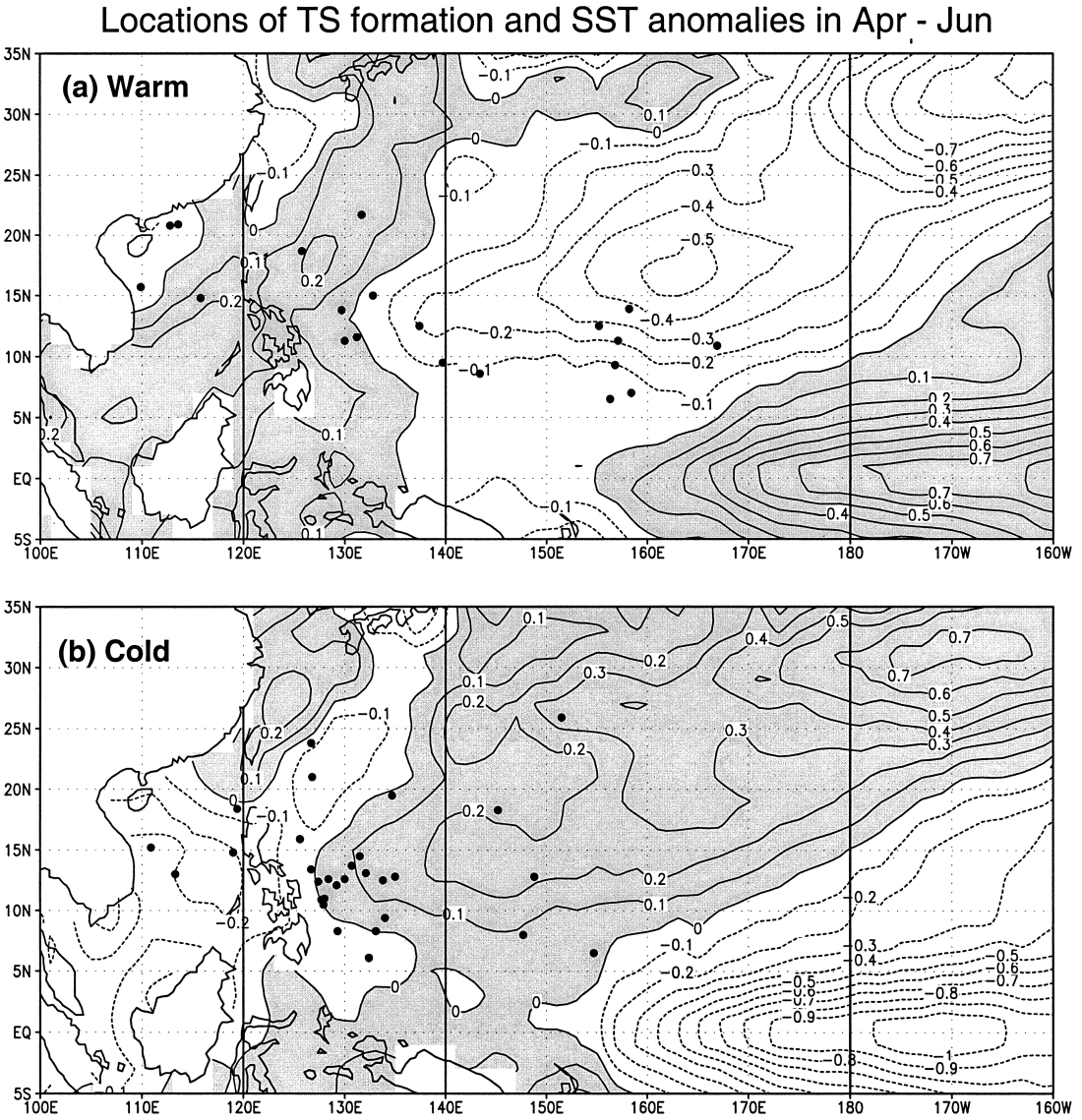

FIG. 3. Locations of initial TS formation and SST anomalies (contours with units of °C) in AMJ during the (a) strong warm and (b) strong cold years (see Table 1). Straight solid lines indicate boundaries of subregions mentioned in the text.

peak and late season (July–December), the mean location of TS formation in the strong warm years is 5° latitude and 11° longitude southeast of that in the strong cold years (Fig. 6c).

Because of the contribution from the extreme events, the seasonal mean latitude of TS formation during the peak season is highly correlated with the Niño-3.4 SST anomaly (correlation coefficient $r = -0.80$; Fig. 7a). The mean longitude of TS formation during the late season is also significantly correlated with the SSTA in the Niño-3.4 regions ($r = 0.69$).

b. Number of TS formations

The total number of TS *formations* averaged for the seven strongest El Niño years is 22.7 and for the seven strongest La Niña years is 20.1. Thus, even between the strong El Niño and La Niña years, the yearly mean number of TS formations is not significant. However, the numbers of TS formations in the SE and NW quadrants are highly correlated with the Niño-3.4 SSTA. During the peak season, for instance, the linear correlation coefficient between the Niño-3.4 SSTA and the number of TS formation in the SE quadrant reaches 0.82 (Fig. 7b), and that in the NW quadrant is -0.61.

c. Mean life span and frequency of TS occurrence

For each individual year, the mean life span is defined by the average time intervals of existence of all TSs that occurred in the peak and late (JASOND) season. Comparing the seven warmest years (1972, 1982, 1986,

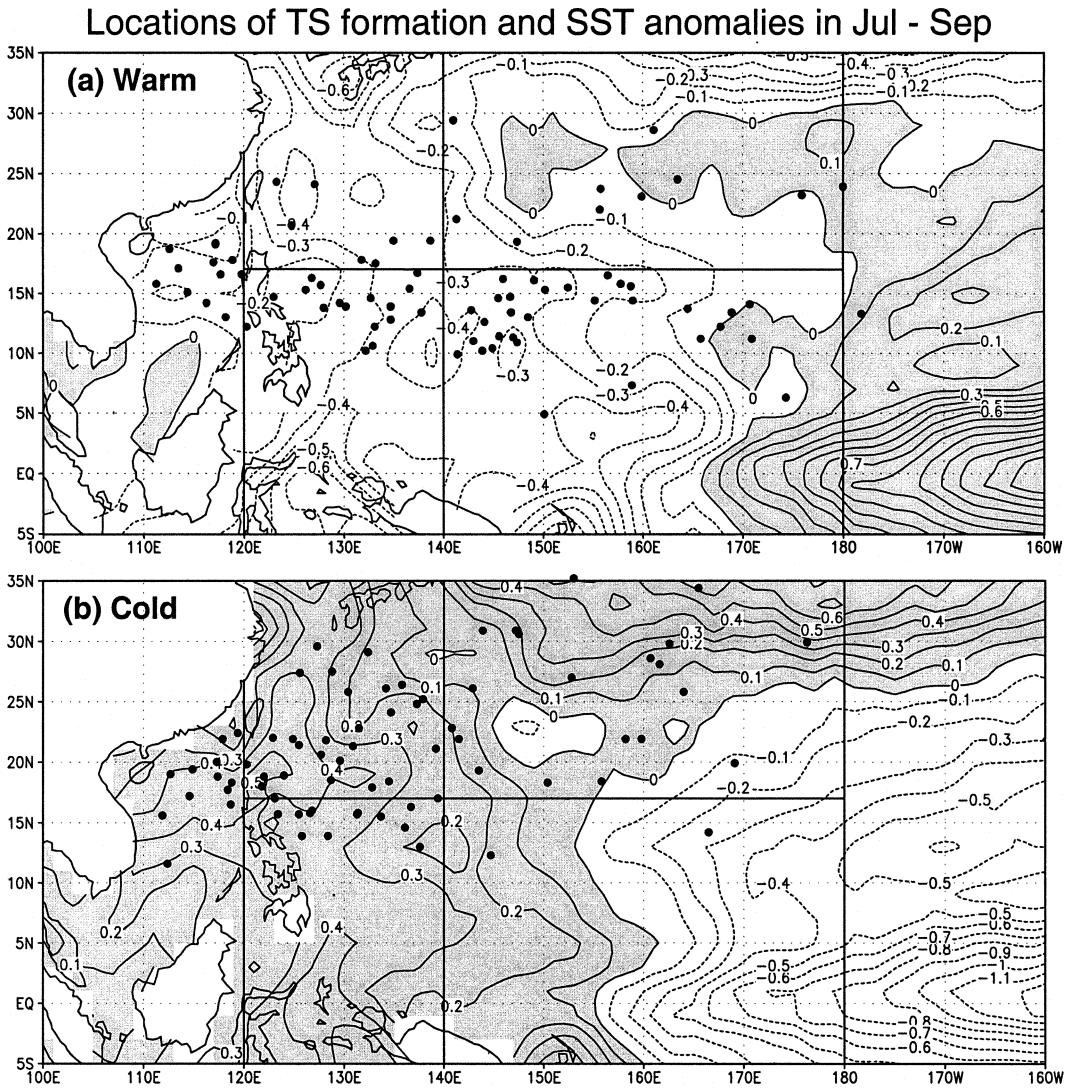

FIG. 4. As in Fig. 3 except for the peak (JAS) season.

1987, 1991, 1994, and 1997) and seven coldest years (1970, 1973, 1974, 1975, 1988, 1998, and 1999) (based on the July–December mean SSTA in the Niño-4 region),[1] the mean number of days of TS occurrence for the warmest years (158.5 days) is nearly twice that for the cold years (84.3 days). The mean life span is 7 days for warm years versus 4.1 days for cold years. For all the years in the data sample, the mean life span tends to increase with increasing Niño-3.4 SSTA (Fig. 7c).

We found that the life span and the location of TS formation are intimately related. Most long-lived (life span exceeding 7 days) TSs form in the *southeast quadrant* of the WNP as shown by the heavy dots in Figs. 8a,b. The frequency of formation of the long-lived TSs in the southeast quadrant during the strong warm years is about 5 times that during the strong cold years. The TSs formed in the southeast quadrant live longer because they tend to be more intense and to have a longer traveling time (westward or northward) before encountering the continent or colder midlatitude water.

d. The tracks

Figure 8c shows the difference between the strong warm and cold years in the SON mean frequency of TS occurrence in each 2.5° lat × 2.5° lon box. The maximum differential frequency of occurrence is used to infer the difference in their prevailing tracks. During warm years, there is a significant increase in the northward recurving TSs, which form in the SE quadrant of the WNP and tend to recurve from northwestward to northeastward around 28°N, 135°E. The total number of TSs reaching north of 35°N is 28 in the strong warm years while only 11 do so in the strong cold years. In

[1] A similar result is obtained using the SSTA in the Niño-3.4 region.

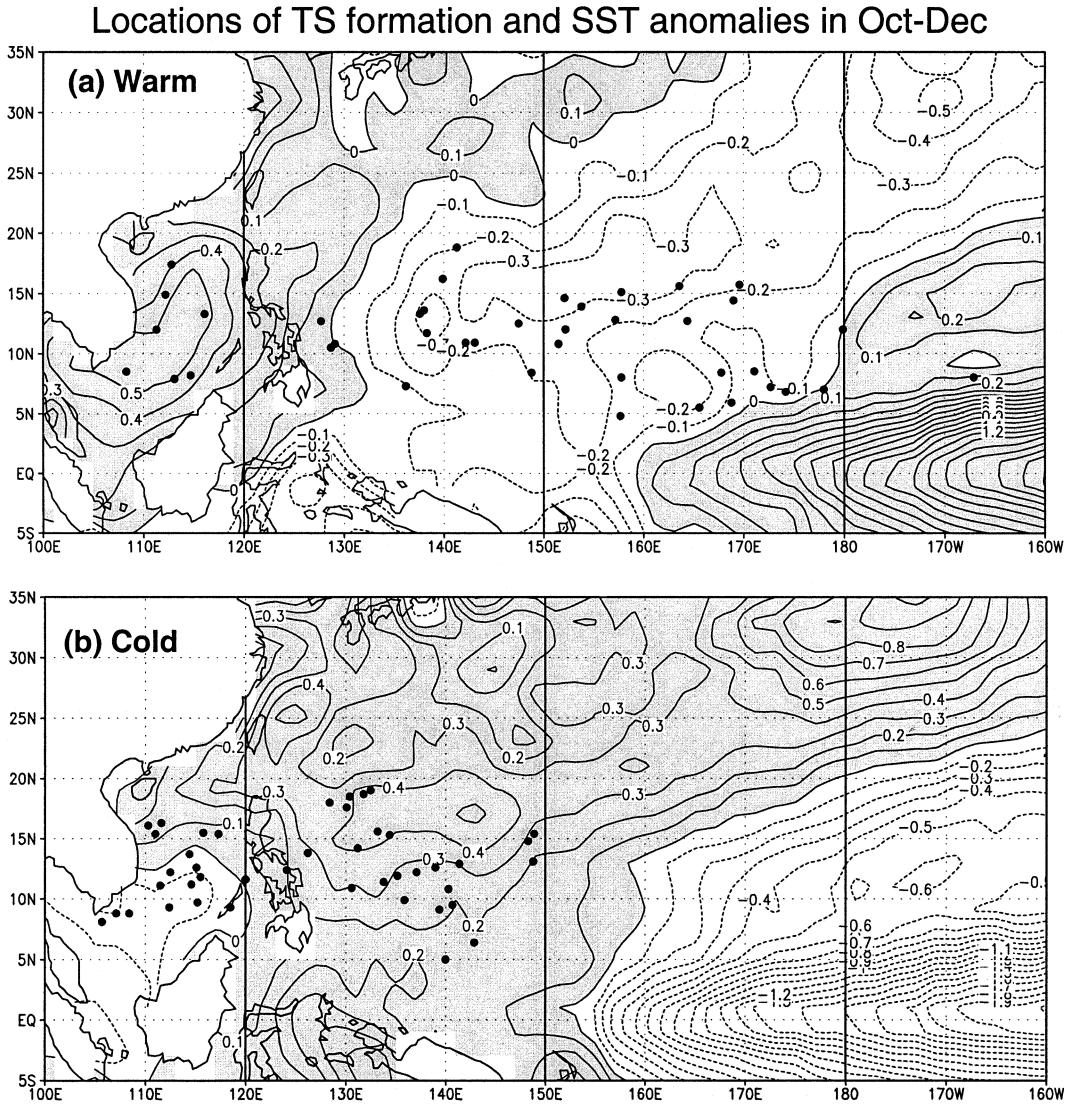

FIG. 5. As in Fig. 3 except for the late (OND) season.

addition, the frequency of a northwestward path toward Taiwan is significantly higher than that during the strong cold years.

4. Interpretation

The local SST anomalies were thought to be a factor that influences the TS formation on interannual timescales (Li 1988). However, Figs. 3, 4, and 5 show clearly that the locations of TS formation do not depend on the signs of local SST anomalies. This is because deep convection depends on the total SST with a critical value of 28°C (Graham and Barnett 1987). During summer, the SST fluctuation in the tropical WNP rarely reaches a strength that brings down the total SST below 28°C. This fact implies that atmospheric dynamics play a fundamental role in determining seasonal mean TS formation.

Gray (1984) used vertical shear as an indicator for prediction of the Atlantic hurricane genesis. Examination of the TS formation in the SE and NW quadrants indicates that in the WNP the likelihood of TS formation cannot be explained by changes in the sign or magnitude of the ENSO-induced vertical shear (figure not shown).

To explain how SST anomalies in the equatorial eastern-central Pacific affect TS activity in the WNP, changes of the seasonal mean circulation at the lower (850 hPa), mid- (500 hPa), and upper (200 hPa) troposphere are presented in Fig. 9. The anomalous circulation composed for the cold episodes are found to be nearly mirror images of those composited for the warm counterparts. To save space, only the differences between the strong warm and cold composites are discussed and the results are simply regarded as warm composites with a doubling amplitude. It should be mentioned that, although the seasonal mean circulation anomalies include the non-

TABLE 2. Contingency tables for the observed numbers of TS formation during warm and cold years in subregions of the WNP. Values of chi-square for each season are given along with the corresponding degree of freedom and the threshold values of chi-square at the 1% confidence level.

(a) Early season (AMJ)

	120°–140°E	140°E–180°	Total
Warm	8	8	16
Cold	21	5	26
Total	29	13	42
$\chi^2 = 4.39$	Degrees of freedom = 1		χ^2 (5%) = 3.84

(b) Peak season (JAS)

	NW quadrant (north of 17°N 120°–140°E)	NE quadrant (north of 17°N 140°E–180°)	SW quadrant (south of 17°N 120°–140°E)	SE quadrant (south of 17°N 140°E–180°)	Total
Warm	7	10	17	31	65
Cold	28	15	12	2	57
Total	35	25	29	33	122
$\chi^2 = 39.61$		Degrees of freedom = 3		χ^2 (1%) = 11.34	

(c) Late season (OND)

	100°–120°E	120°–150°E	150°E–180°	Total
Warm	7	13	20	40
Cold	18	25	0	43
Total	25	38	20	83
$\chi^2 = 28.55$	Degrees of freedom = 2		χ^2 (1%) = 9.21	

linear rectification of the transient TS activity, the modification of the mean fields by the transients should not be a dominant factor. This is because the spatial scales and timescales of TSs are an order of magnitude smaller than the large-scale mean circulation, and the influence of tropical cyclones is by and large offset by the complementary circulation anomalies surrounding the cyclones. For simplicity, the observed circulation anomalies are considered to result primarily from the steady response of the circulation to the anomalous ENSO forcing.

Because the vertical motion-induced cooling in the Tropics is primarily balanced by diabatic heating on the seasonal mean timescale, the ascending (descending) motion is a meaningful indication for atmospheric heat source (sink). Figure 9b shows that during the strong warm years, the organized anomalous ascending motion concentrates in the SE quadrant of the WNP (defined in Fig. 4), whereas anomalous descending motion is found in the NW quadrant. The amplitudes of these anomalies reach 40%–50% of the climatological means. This dipole heat source pattern enhances TS formation in the SE quadrant while it suppresses formation in the NW quadrant during the warm years.

We argue that the anomalous heat source pattern in the WNP results from the lower boundary forcing associated with equatorial SST anomalies. During the warm years, the equatorial central and eastern Pacific warming increases equatorial convective heating near the date line and induces pronounced equatorial westerly anomalies in the western Pacific. Large meridional shears associated with the equatorial westerly anomalies increase low-level vorticity in the SE quadrant. Since the boundary layer Ekman convergence is proportional to the 850-hPa relative vorticity, the background vertical motion is well correlated with the 850-hPa vorticity ($r = -0.80$; Fig. 10a). The increase of the background low-level vorticity would help spin up tropical cyclones by increasing moisture convergence and by entraining potential vorticity into tropical cyclones. As a result, the SE quadrant favors for TC intensification. The high correlation coefficient ($r = 0.72$ for 1965–99) between

TABLE 3. Mean deviations in the TS formation location (lon and lat) of strong warm, moderate warm, moderate cold, and strong cold years. Positive (negative) values indicates eastward (westward) in lon and northward (southward) in lat. The bold letters indicate that the difference is statistically significant at 5% confidence level by the two-sample *t* test.

	JAS		OND		Jul–Dec	
Mean deviation	Lat	Lon	Lat	Lon	Lat	Lon
Strong warm years	**−2.5**	**5.8**	**−1.5**	**9.4**	**−2.7**	**6.7**
Moderate warm years	−0.1	**3.7**	−0.7	0.9	−1.1	2.4
Moderate cold years	**2.2**	−0.2	0.5	−4.6	0.1	−1.1
Strong cold years	**3.8**	−2.6	0.5	**−8.5**	**2.4**	**−4.5**

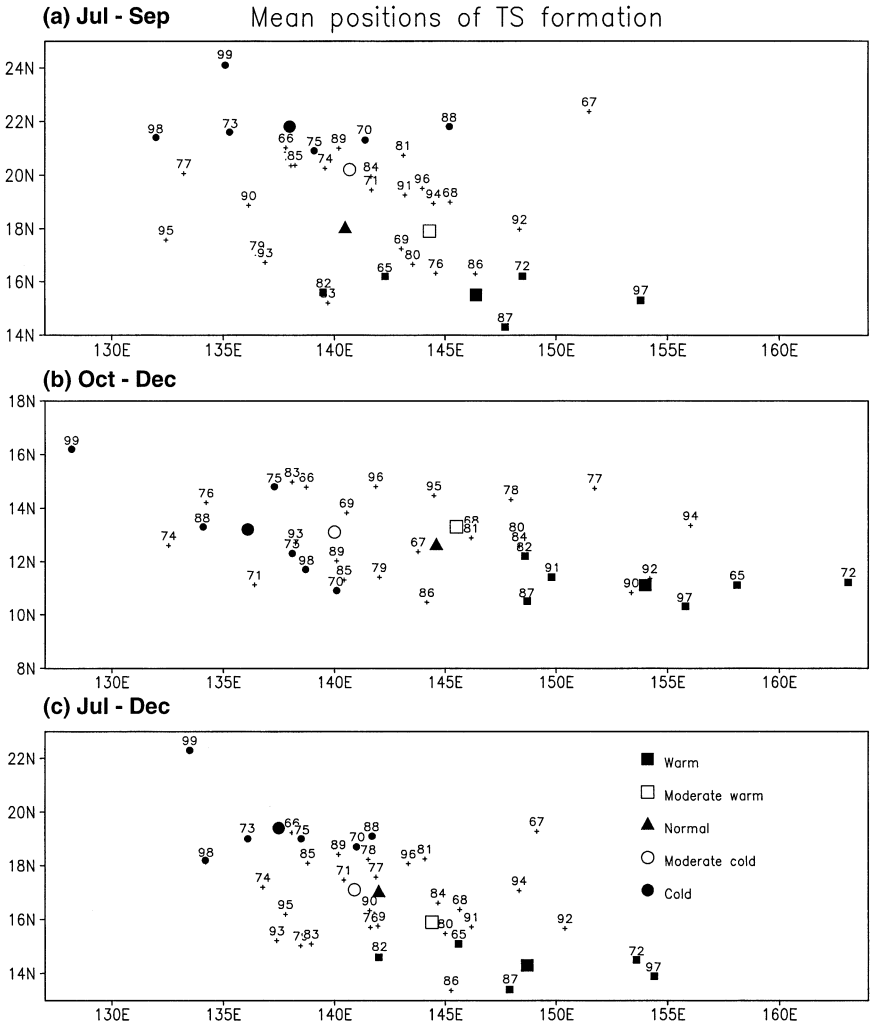

FIG. 6. The averaged locations of TS formation during (a) JAS, (b) OND, and (c) Jul–Dec of each year from 1965 to 1999. Heavy squares and solids denote strong warm and strong cold years, respectively. The mean locations of TS formation for each of the five categories of SST anomalies are marked by large-size symbols as shown in (c).

the background 850-hPa vorticity and the frequency of TS formation in the SE quadrant (Fig. 10a) supports this argument.

The El Niño–induced central Pacific heating also generates a pair of huge anomalous anticyclones in the upper levels that resides on each side of the equator due to equatorial wave adjustment in the tropical atmosphere (Fig. 9c). Over east Asia, the upper-level troughs at 500 and 200hPa are deeper than normal during the El Niño fall (Figs. 9b and 9c). The deepening appears to result from land surface cooling during the El Niño summer over northeast Asia (Wang and Zhang 2001, manuscript submitted to *J. Climate*). Thus, the northwesterly behind the east Asian trough and the anomalous southeasterly behind the subtropical anticyclone generate strong upper-level convergence in the NW quadrant (Fig. 9c). The latter appears to be a major cause of the observed descending motion (Fig. 9b), which suppresses tropical cyclone intensification in the NW quadrant. The 200-hPa divergence is a reasonable indicator for the number of TS formations in the peak season ($r = 0.61$; Fig. 10b). The deepening of the east Asian trough in the midtroposphere also provides a favorable anomalous steering flow for the TS recurvature around 135°E.

5. Physical basis for prediction of the WNP TS activity

The simultaneous correlations shown in Fig. 7 can be used for skillful seasonal forecasts provided that the equatorial SST anomalies can be predicted in advance. Here we propose simple empirical schemes for predicting Niño-3.4 SSTA, hence the TS activity, and discuss the physical basis for such schemes.

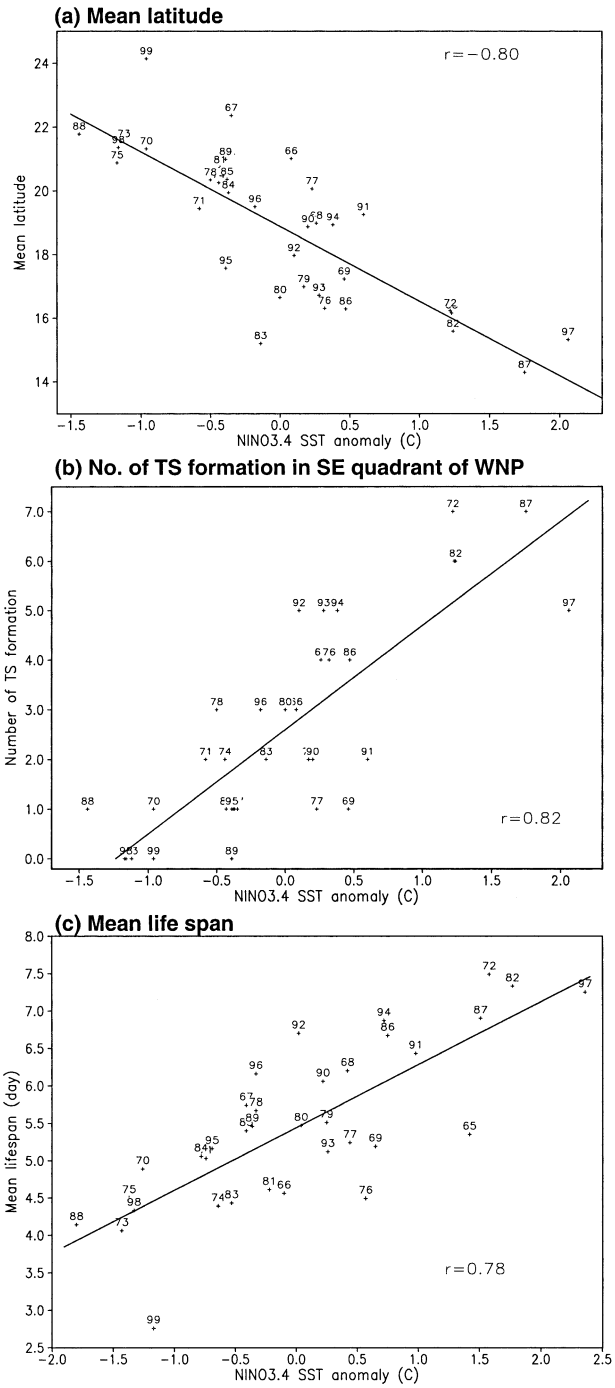

FIG. 7. (a) Correlation of the mean latitudes of the TS formation in JAS with the Niño-3.4 SSTA. In (b) as in (a) except for the number of TS formations in the southeast quadrant of the WNP (5°–17°N, 140°–180°E). In (c) as in (a) except for the mean TS life span in the entire WNP (0°–30°N, 120°–180°E) during Jul–Dec. The linear correlation coefficients and regression lines are given in each panel.

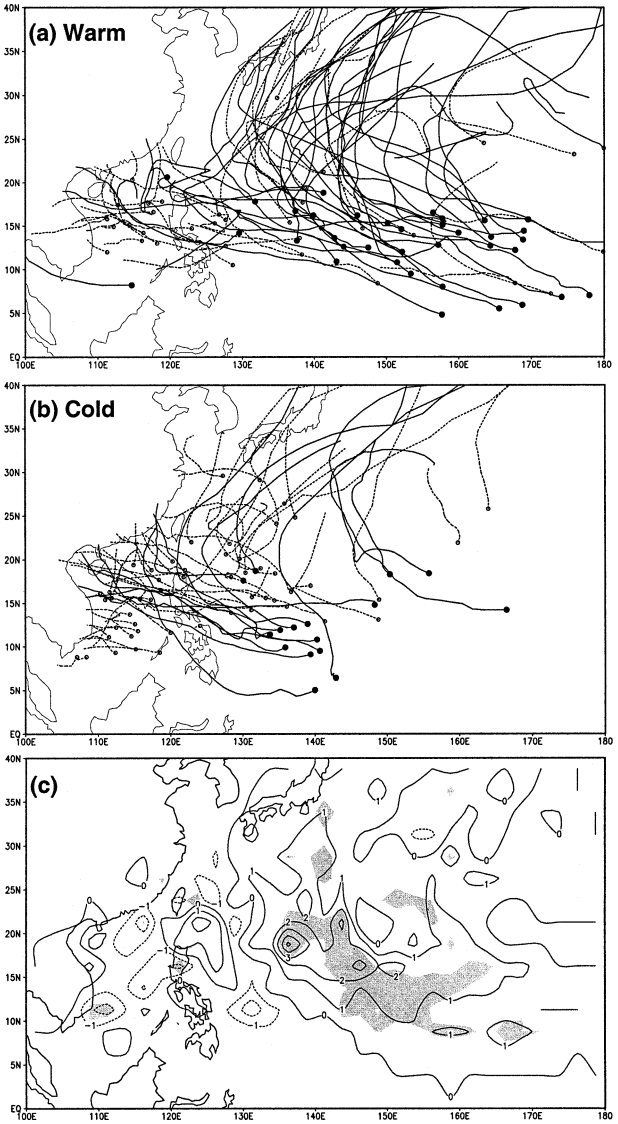

FIG. 8. (a) SON TS tracks during the six strongest warm years (1965, 1972, 1982, 1987, 1991, and 1997). The locations (tracks) of the long-lived (life span exceeding 7 days) tropical storms formation are marked by heavy solid dots (solid lines). Locations (tracks) of other storms are denoted by open circle (dashed lines). (b) The same as in (a) but for the six strongest cold years (1970, 1973, 1975, 1988, 1998, and 1999). (c) The difference in the total number of TS occurrence in each 2.5 lat × 2.5 lon grid during SON between the strong warm and cold years. Shading indicates areas where the difference is statistically significant at the 1% confidence level by the two-sample *t* test.

a. Peak and late season (July–December) TS activity

The JAS SST anomalies may be predicted by simple linear extrapolation:

$$\text{SSTA (JAS)} = 2\ \text{SSTA (AMJ)} - \text{SSTA (JFM)}. \quad (5.1)$$

The correlation coefficient between the predicted and observed Niño-3.4 SSTA is 0.88 for the 35-yr period (1965–99), that is, about 78% of the total variance can be captured using this simple formula. More generally, one may use AMJ mean SSTA and the SST tendency, DX = AMJ mean SST minus JFM mean SST, as two

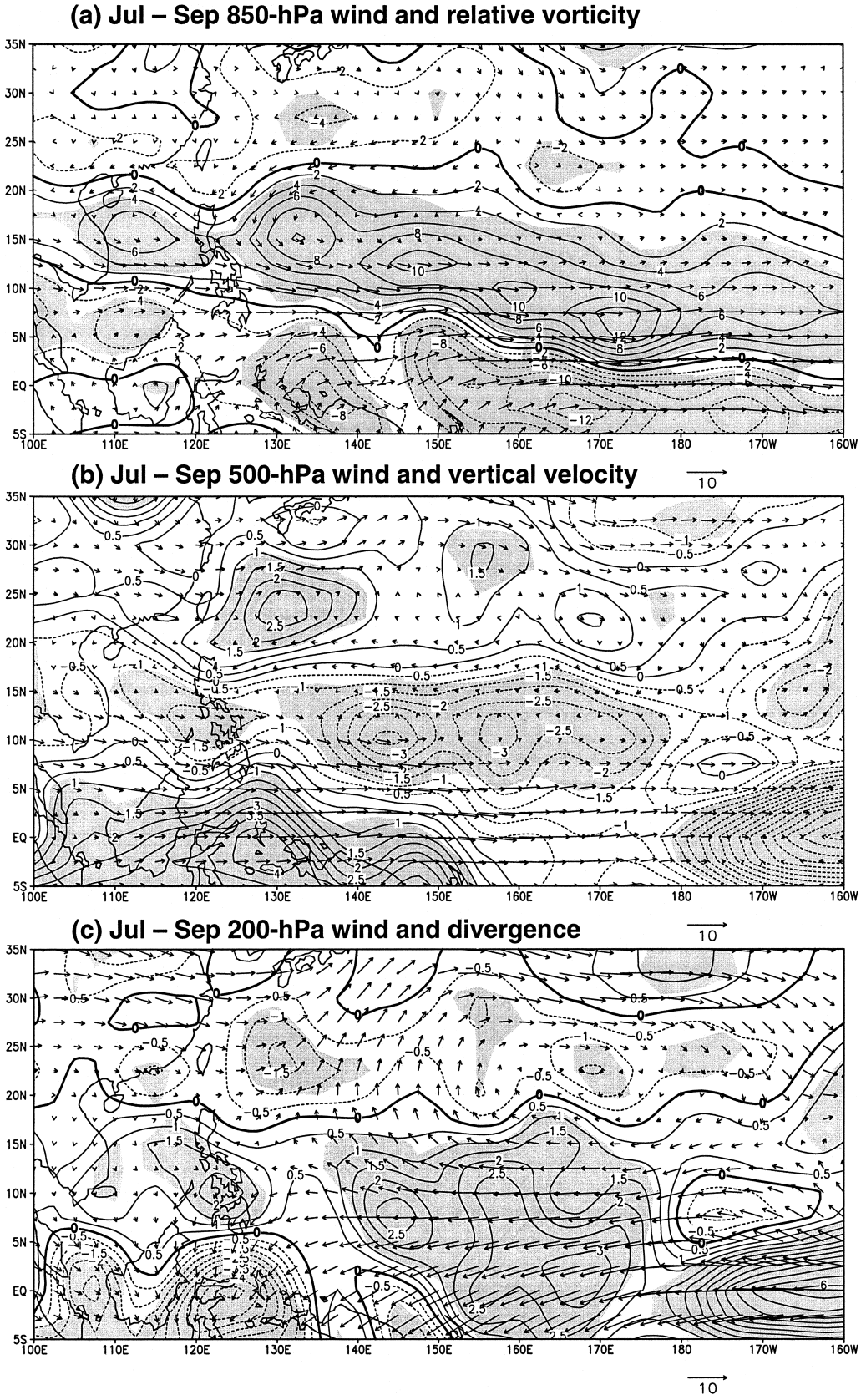
(a) Jul – Sep 850-hPa wind and relative vorticity
(b) Jul – Sep 500-hPa wind and vertical velocity
(c) Jul – Sep 200-hPa wind and divergence
10
35N
30N
25N
20N
15N
10N
5N
EQ
5S
100E
110E
120E
130E
140E
150E
160E
170E
180
170W
160W

predictors to derive a multiregression equation for prediction of the subsequent seasonal mean SSTA:

$$\text{SSTA(JAS)} = 0.91\text{SSTA(AMJ)} + 0.59\text{DX}, \quad (5.2a)$$

$$\text{SSTA(OND)} = 0.86\text{SSTA(AMJ)} + 1.17\text{DX}, \quad (5.2b)$$

$$\text{SSTA(Jul–Dec)} = 1.05\text{SSTA(AMJ)} + 0.77\text{DX}. \quad (5.2c)$$

The correlation coefficients between the predicted and observed SST anomalies for JAS, OND, and July–December are, respectively, 0.91, 0.86, and 0.89.

The physical basis for such a reliable extrapolation is simple. The El Niño–Southern Oscillation (ENSO) warming or cooling tends to peak toward the end of the calendar year. Therefore, in the transition and development phases of an ENSO cycle, which normally occur from early spring to the end of the calendar year, a linear extrapolation can well catch the tendency of the equatorial Pacific SSTA by taking advantage of the strong phase-locking property of ENSO.

The phase-locking property of ENSO allows us to predict TS activity in the peak and late TS seasons by using the preceding spring and winter SSTAs. Such a possibility is demonstrated by the significant correlation coefficients between the predicted SSTA and various indexes that depict tropical storm activities (Table 4). One may further improve these predictions. For instance, use of DJF and MAM SSTAs to predict SSTAs in JAS and OND may provide a longer lead for climate forecast.

b. *January–July storm activity*

Lander (1994) found that the number of early season (March to mid-July) storms in the WNP is strongly related to the *change* of the Niño-3 SSTA between January–April and May–August ($r = 0.65$ for 1970–1991). This simultaneous correlation implies that during a *rapid* development of El Niño (La Niña), more (less) storm form in the early season (see Fig. 2). It is difficult to use this simultaneous relationship for prediction, because it requires an accurate forecast of the rate of change in Niño-3 SST, which is more difficult than prediction of Niño-3 SSTA itself.

Different from Lander, we found that in the year after a strong El Niño (e.g., 1966, 1973, 1983, 1988, 1992, and 1998), the January–July total number of TS formation over the WNP is lower than normal (6/6), whereas after the strong La Niña (e.g., 1971, 1974, 1976, 1989, and 1999), the January–July TS formation tends to be above normal (4/5). Because the El Niño (La Niña) tends to mature toward the end of the calendar year (Rasmusson and Carpenter 1982), by using the preceding OND mean Niño-3.4 SSTA, one can predict the early season TS formation number. Such a negative lag correlation is shown in Fig. 11a. The prediction works well after strong El Niño and La Niña events occur. When the OND SST is warmer than 0.5°C (total 12 yr), the TS formation number in the following January–Jul are all below normal. For strong cold events (say the OND SSTA < -1.0°C), the TS formation number in the following January–July tends to be high (6/7).

What is the physical basis for such predictability? Wang et al. (2000) recently found that before the peak phase of El Niño, a low-level anomalous anticyclone establishes over the Philippine Sea. Conversely, after a peak La Niña, an anomalous cyclone dominates the Philippine Sea. The anticyclonic (cyclonic) anomaly then persists until the ensuing summer. Thus, during the spring and summer after the peak warming, the anom-

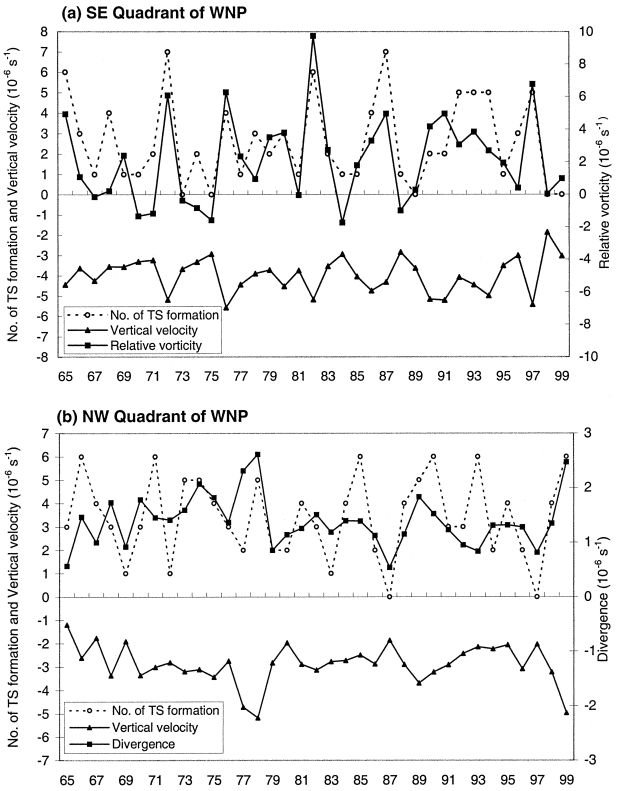

FIG. 10. (a) Time series of JAS mean 850-hPa relative vorticity, 500-hPa vertical p velocity, and total numbers of TS formation in the southeast quadrant of the WNP (5°–17°N, 140°E–180°) from 1965 to 1999. (b) Time series of JAS mean 200-hPa divergence, 500-hPa vertical p velocity, and total number TS formation in the northwest quadrant WNP (17°–30°N, 120°–140°E) from 1965 to 1999. The units for vorticity, p velocity, and divergence are, respectively, 10^{-6} s^{-1}, 10^{-2} Pa s^{-1}, and 2×10^{-6} s^{-1}.

←

FIG. 9. (a) Difference (strong warm minus strong cold years) in JAS mean 850-hPa winds (vector) and relative vorticity (contours). Units for winds are m s^{-1} and for vorticity 10^{-6} s^{-1}. (b) As in (a) except for 500-hPa winds (m s^{-1}) and vertical pressure velocity (10^{-2} Pa s^{-1}). (c) As in (a) except for 200-hPa winds and divergence.

TABLE 4. Correlation coefficients of predicted Niño-3.4 SST anomaly with a number of TS activity indices. For comparison, the corresponding correlation coefficients with observed Niño-3.4 SST anomaly are also given.

Tropical storm activity indexes	Observed Niño-3.4 SSTA	Predicted Niño-3.4 SSTA
JAS TS formation number in the SE quadrant	0.82	0.76
JAS mean latitude of TS formation in WNP	−0.80	−0.75
Jul–Dec mean longitude of TS formation in WNP	0.68	0.62
Jul–Dec mean life span of TS in WNP and SCS	0.78	0.70
Jul–Dec total number of TS occurrence in WNP	0.63	0.62

alous Philippine Sea anticyclone provides large-scale subsidence. Results shown in Fig. 11b confirm this finding. The 500-hPa vertical velocity anomalies over the Philippine Sea (10°–20°N, 130°–150°E) averaged for the period from January to July is indeed highly correlated with the Niño-3.4 SST anomaly in the previous OND. Therefore, the TS formation in the same period must be suppressed due to the large-scale background subsidence.

We note that the chaotic atmosphere itself cannot maintain the wind anomalies over the Philippine Sea.

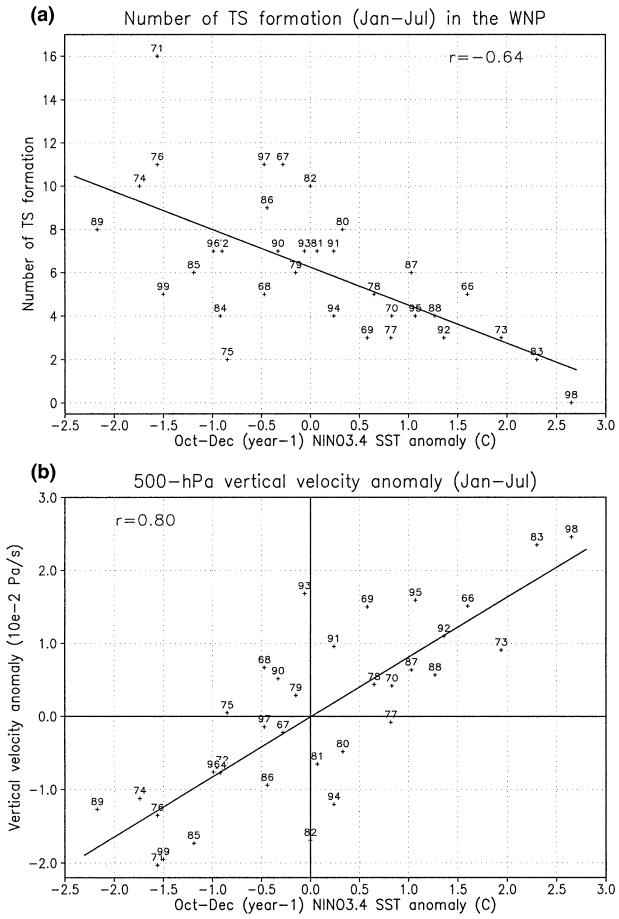

FIG. 11. (a) Number of tropical storm formations in the WNP (0°–30°N, 120°E–180°) during Jan–Jul. (b) Jan–Jul mean 500-hPa vertical pressure velocity averaged over (10°–20°N, 130°–150°E) as functions of Niño-3.4 SST anomalies in OND of the preceding year.

Although the establishment of the Philippine Sea anticyclone results from the ENSO forcing, its maintenance cannot be explained by the remote ENSO forcing, because by the ensuing summer, the positive Niño-3.4 SSTA either disappears or turns to negative (in the case of July 1998, for example). The maintenance mechanism is attributed to a local positive feedback between atmospheric Rossby waves and ocean mixed-layer thermodynamics (Wang et al. 2000), which is briefly stated as follows. To the east of the anomalous Philippine Sea anticyclone, the total wind speed increases in the presence of background northeasterly trades/monsoon, leading to negative SST anomalies due to enhanced evaporation and entrainment. The negative SST anomalies reduce convective latent heat release, which generates anomalous westward-propagating descending Rossby waves. These Rossby waves would in turn reinforce the low-level Philippine Sea anticyclone. This positive local air–sea feedback would maintain both the anticyclone and negative SST anomalies in the WNP.

6. Summary

Analyses of 35-yr (1965–99) tropical storm (TS) activity over the western North Pacific (WNP) lead to a number of new findings on the year-to-year variation of the tropical storm activity.

The relationship between the WNP TS activity and ENSO strongly depends on the intensity of ENSO episodes. Strong El Niño or La Niña events (Niño-3.4 SST anomaly exceeds 1 std dev) have significant impacts on the WNP TS activity, but the moderate warm (cold) events do not show definite significant impacts. Without distinguishing the impacts between moderate and strong events, one would overestimate the effects of moderate events and underestimate the impacts of the strong events. For this reason, we quantify, in general, only the impacts of the strong El Niño and La Niña.

In contrast to the common practice in long-term typhoon prediction (forecast of the total number of TC formation in the entire WNP domain), we confirmed that the total number of TS formation in the entire WNP does not show significant ENSO influence. However, we identify two subregions where largest variability occurs in close association with strong ENSO events: the SE (17°–30°N, 120°–140°E) and NW (17°–30°N, 120°–140°E) quadrants. The longitudinal division between the

SE and NW quadrants (140°E) differs from the longitude that was previously recognized for the eastward shift of the formation longitude (160°E). Our results suggest that one should not forecast the total number of TS formations in the entire WNP domain, rather, they should predict those in the SE and NW quadrants.

We found that the mean TS *life span* is about 7 (4) days and the mean *total number of TS occurrences* is 159 (84) days in strong warm (cold) years. This conclusion allows us to estimate the total days (or frequency) of occurrence of TS over the entire WNP domain. We also showed that the TS tracks differ substantially between the strong warm and cold years. During El Niño fall, the number of TS that formed south of 15°N and recurved northward across 35°N is 2.5 times that during cold years. This fact implies that the meridional exchange of heat and energy is greatly enhanced during the strong El Niño years. This is a critical process by which El Niño conveys its impacts to high latitudes and enhances interaction between the Tropics and extratropics in the east Asia–WNP.

During strong El Niño (La Niña) years, the TS formation in the SE and NW quadrant exhibits a dipole anomaly pattern with enhanced (suppressed) formation in the SE (NW) quadrant. In consistence with the dipole pattern, the JAS *mean location* of TS formation is 6° latitude lower, while that in OND is 18° longitude eastward during strong El Niño compared with strong La Niña.

Our explanation focused on two issues that were rarely discussed in the literature. The first issue concerns with the cause of SE–NW dipole pattern in the peak season TS formation. We propose that the low-level shear vorticity associated with equatorial westerlies is a fundamental cause for the enhanced generation in the SE quadrant, while the upper-level divergence induced by the deepening of east Asian trough and strengthening the WNP subtropical high, both resulting from El Niño forcing, suppresses TS generation over the NW quadrant of the WNP. The second issue is concerned with the cause of the variability of the January–July TS formation. We pointed out that the delayed El Niño impacts to early season TS activity in the year following peak El Niño is due to the persistence of the Philippine Sea anticyclone, which is set up during the mature phase of El Niño but maintained through the subsequent spring and summer by the local positive feedback between the Philippine Sea anticyclonic anomaly and the mixed-layer ocean thermodynamics.

Because the peak warm and cold phases tend to occur toward the end of the calendar year, during the year in which an El Niño or La Niña develops, the Niño-3.4 SSTA in the peak and late TS season can be predicted by simple linear extrapolation using preceding winter and spring SSTA. This forms a physical basis for seasonal prediction of WNP TS activity one or two seasons ahead. After the mature phase of El Niño (La Niña), the Philippine Sea is dominated by an anticyclonic (cyclonic) circulation anomalies, thus the TS activity is suppressed (enhanced). This makes it possible to forecast the early season TS activity using the Niño-3.4 SSTA in the preceding late fall.

In the present study, we used TS formation to measure the TC intensification, because the number of typhoon formations is significantly less, while the determination of the tropical depression formation is less accurate due to the limitation of observations. However, we expect that the physical processes that govern the TS formation should be applicable to the interpretation of the variability in typhoon or tropical depression formation. But additional analyses are needed to verify this assertion. We are looking for the common features in the ENSO–TS relationship in the WNP. Decadal trends or variations in TS formation are not a primary concern. Since the strong El Niño years (1965, 1972, 1982, 1987, 1992, and 1997) and La Niña years (1970, 1973, 1975, 1988, 1998, and 1999) occur both before and after 1979, our analysis would not be significantly affected by decadal trend. However, the decadal changes in TS activity over the WNP deserve further investigation.

Acknowledgments. We thank Mr. Jian Hu for his participation in a part of the early analysis and Mr. K. S. Liu who helped in most of the data processing and figure preparation. Dr. Alexis Lau provides constructive comments during BW's presentation of an early version of this manuscript. This study is supported by the Marine Meteorology Program of the Office of Naval Research. Much of the work of BW was accomplished during his visit to the City University of Hong Kong, which was supported by the Research Enhancement Scheme and Grant 7010010, both of the City University of Hong Kong. The International Pacific Research Center is sponsored in part by the Frontier Research System for Global Change.

REFERENCES

Atkinson, G. D., 1977: Proposed system for near real time monitoring of global tropical circulation and weather patterns. Preprints, *11th Tech. Conf. on Hurricanes and Tropical Meteorology,* Miami Beach, FL, Amer. Meteor. Soc., 645–652.

Chan, J. C. L., 1985: Tropical cyclone activity in the northwest Pacific in relation to the El Niño/Southern Oscillation phenomenon. *Mon. Wea. Rev.,* **113,** 599–606.

——, 1994: Prediction of the interannual variations of tropical cyclone movement over regions of the western North Pacific. *Int. J. Climatol.,* **14,** 527–538.

——, 2000: Tropical cyclone activity over the western North Pacific associated with El Niño and La Niña events. *J. Climate,* **13,** 2960–2972.

——, J. E. Shi, and C. M. Lam, 1998: Seasonal forecasting of tropical cyclone activity over the western North Pacific and the South China Sea. *Wea. Forecasting,* **13,** 997–1004.

Chen, T.-C., S.-P. Weng, N. Yamazaki, and S. Kiehne, 1998: Interannual variation in the tropical cyclone formation over the western North Pacific. *Mon. Wea. Rev.,* **126,** 1080–1090.

Dong, K., 1988: El Niño and tropical cyclone frequency in the Australian region and the northwest Pacific. *Aust. Meteor. Mag.,* **36,** 219–225.

Dvorak, V. F., 1975: Tropical cyclone intensity analysis and forecasting from satellite imagery. *Mon. Wea. Rev.,* **103,** 420–464.
——, 1984: Tropical cyclone intensity analysis using satellite data. NOAA Tech. Rep. NESDIS 11, 47 pp.
Graham, N. E., and T. P. Barnett, 1987: Sea surface temperature, surface wind divergence, and convection over tropical oceans. *Science,* **238,** 657–659.
Gray, W. M., 1984: Atlantic seasonal hurricane frequency. Part II: Forecasting its variability. *Mon. Wea. Rev.,* **112,** 1669–1683.
Japanese Meteorological Agency, 1991: Atmospheric and oceanic conditions in the tropics and tropical cyclones in 1991. Annual Report on Activities of the RSMC Tokyo-Typhoon Center 1991, Japanese Meteorological Agency, 7–9.
Kalnay, E., and Coauthors, 1996: The NCEP/NCAR 40-Year Reanalysis Project. *Bull. Amer. Meteor. Soc.,* **77,** 437–471.
Kang, I.-S., Y.-M. Lee, and S.-I. An, 1995: Interannual variability of Typhoon activity over the western North Pacific and El Niño. *J. Korean Meteor. Soc.,* **31,** 15–26.
Lander, M. A., 1993: Comments on ''A GCM simulation of the relationship between tropical storm formation and ENSO.'' *Mon. Wea. Rev.,* **121,** 2137–2143.
——, 1994: An exploratory analysis of the relationship between tropical storm formation in the western North Pacific and ENSO. *Mon. Wea. Rev.,* **122,** 636–651.
Landsea, C. W., 2000: El Niño–Southern Oscillation and the seasonal predictability of tropical cyclones. *El Niño: Impacts of Multiscale Variability on Natural Ecosystems and Society,* H. F. Diaz and V. Markgraf, Eds., 149–181.
Li, C., 1988: Actions of typhoon over the western Pacific (including the South China Sea) and El Niño. *Adv. Atmos. Sci.,* **5,** 107–115.
Ramage, C. S., and A. M. Hori, 1981: Meteorological aspects of El Niño. *Mon. Wea. Rev.,* **109,** 1827–1835.
Rasmusson, E. M., and T. H. Carpenter, 1982: Variations in tropical sea surface temperature and surface wind fields associated with the Southern Oscillation/El Niño. *Mon. Wea. Rev.,* **110,** 354–384.
Wang, B., and T. Li, 1993: A simple tropical atmospheric model of relevance to short-term climate variation. *J. Atmos. Sci.,* **50,** 260–284.
——, R. Wu, and X. Fu, 2000: Pacific–East Asian teleconnection: How does ENSO affect East Asian climate? *J. Climate,* **13,** 1517–1536.
Wilks, D. S., 1995: *Statistical Methods in the Atmospheric Sciences.* Academic Press, 467 pp.
Wu, G., and N.-C. Lau, 1992: A GCM simulation of the relationship between tropical-storm formation and ENSO. *Mon. Wea. Rev.,* **120,** 958–977.